Korean J. Chem. Eng., 40(2), 429-435 (2023)
DOI: 10.1007/s11814-022-1348-0

pISSN: 0256-1115
eISSN: 1975-7220

A high-sensitivity cfDNA capture enables to detect the BRAF V600E mutation in papillary thyroid carcinoma

Tae Hee Lee*,,‡, Hong Jae Jeon***,‡, Jung Hyun Choi****,‡, Young Jun Kim*****, Pil-Neo Hwangbo**, Hyun Sung Park****, Chae Yeon Son****, Hei-Gwon Choi******,*******, Ha Neul Kim******,*******, Jae Won Chang********, Jiyoon Bu****,*********,†, and Hyuk Soo Eun*********,**********,†**

*Department of Biomedical Laboratory Science, Daegu Health College, Chang-ui Building, 15 Yeongsong-ro, Buk-gu, Daegu 41453, Korea
**Industry Academic Cooperation Foundation, Daegu Health College, 15 Yeongsong-ro, Buk-gu, Daegu 41453, Korea
***Department of Internal Medicine, Chungnam National University Sejong Hospital (CNUSH), 20, Bodeum 7-ro, Sejong 30099, Korea
****Department of Biological Sciences and Bioengineering, Inha University, 100 Inha-ro, Michuhol-gu, Incheon 22212, Korea
*****School of Integrative Engineering, Chung-Ang University, Heukseok-dong, Dongjak-gu, Seoul 06974, Korea
******Brain Korea 21 FOUR Project for Medical Science, Chungnam National University, 266, Munwha-ro, jung-gu, Daejeon 35015, Korea
*******Department of Medical Science, Chungnam National University, 266, Munwha-ro, jung-gu, Daejeon 35015, Korea
********Department of Otolaryngology-Head and Neck Surgery, Research Institute for Medical Science, Chungnam National University, 266, School of Medicine, Daejeon 35015, Korea
*********Industry-Academia Interactive R&E Center for Bioprocess Innovation, Inha University, Incheon 22212, Korea
**********Department of Internal Medicine, Chungnam National University Hospital, 282, Daejeon 35015, Korea
**********Department of Internal Medicine, College of Medicine, Chungnam National University, 266, Munwha-ro, jung-gu, Daejeon 35015, Korea
(*Received 1 August 2022 • Revised 12 November 2022 • Accepted 16 November 2022*)

Abstract−Although many efforts have been made to investigate a promising biomarker for the diagnosis of papillary thyroid cancer (PTC), the currently available biomarkers lack the sensitivity to accurately characterize PTC. Here, we established a high-sensitivityt cell-free DNA (cfDNA) detection system using polydopamine-silica (PDA/SiO_2) hybrids to enable clinically reliable analysis of PTC. The PDA/SiO_2-coated beads improved the detection of DNA by 1.76-fold ($p=0.031$) compared to the conventional silica-based cfDNA capture system. The PDA-SiO_2-coated beads were then applied for the detection of cfDNA from serum samples obtained from 37 PTC patients, and the $BRAF^{V600E}$ mutation status in captured DNA was analyzed using both quantitative polymerase chain reaction (qPCR) and digital droplet PCR (ddPCR). The $BRAF^{V600E}$ mutation status analyzed using both assays demonstrated a strong correlation with the multifocality of PTC, exhibiting area under receiver operating characteristic curve (AUC-ROC) of >0.964 ($p<0.001$). In contrast, none of the serum antigens or antibodies related to PTC or thyroid functions exhibited clinically significant prediction for detecting PTC patients with multifocal tumors. These findings suggest that cfDNA capture using PDA/SiO_2-coated beads is a promising approach for analyzing the BRAF mutation, which can serve as an excellent diagnostic biomarker for PTC.

Keywords: ctDNA, cfDNA, Liquid Biopsy, Thyroid Tumor, Papillary Thyroid Cancer

INTRODUCTION

Thyroid cancer is one of the most common malignancies found in endocrine systems. The incidence of thyroid cancer has increased remarkably over the past three decades, and it is known to account for 3% of the global cancer incidence as of 2020 [1,2]. In particular, recent studies have demonstrated the increasing incidence of papillary thyroid carcinoma (PTC) over the past decade [1]. Currently, fine-needle aspiration (FNA) is employed as a gold standard for the diagnosis of PTC, specifically for patients with a high risk of malignancy or a large-sized tumor. The analysis of FNA specimens has been demonstrated to help estimate various malignancies and decide the treatment method for PTC [3]. Specifically, the $BRAF^{V600E}$ mutation is frequently assessed in FNA specimens, especially for patients who are categorized to have atypia of undetermined significance/follicular lesion of undetermined significance (AUS/FLUS) or suspicious for high malignancies.

BRAF mutation is one of the driver mutations in the development of thyroid cancer that is commonly observed in various types

†To whom correspondence should be addressed.
E-mail: jbu@inha.ac.kr, hyuksoo@cnu.ac.kr
‡These authors contributed equally.

of thyroid carcinoma [4]. The mutation is reported to activate the mitogen-activated protein kinase (MAPK) signaling pathway, which facilitates the growth of thyroid carcinoma cells [4]. Despite the variation, one recent study has revealed that the prevalence of $BRAF^{V600E}$ mutation in PTC is greater than 45% [4]. Moreover, several studies have reported that $BRAF^{V600E}$ mutation in surgical specimens is strongly associated with high malignancies for patients with PTC [5-8]. Specifically, patients with PTC having $BRAF^{V600E}$ mutation showed a higher recurrence rate after thyroidectomy and increased cancer-related mortality [5-8]. The $BRAF^{V600E}$ mutation is also utilized as a predictive marker for radioiodine therapy, as well as an indicator for infiltration of the tumoral capsule and the presence of multifocality in PTC [8-10].

Despite its high clinical utility as a biomarker for thyroid cancer, the $BRAF^{V600E}$ mutation analysis based on the specimens obtained from FNA has several limitations. Intra-tumoral heterogeneity is one of the most critical factors that affect the accuracy of FNA-based tumor analysis [11]. Since a large thyroid nodule harbors microcarcinomas, FNA, which analyzes small fragments of tissue, has the potential to misrepresent the genetic and phenotypic characteristics of tumors [12,13]. This can be evidence for the higher false-negative rate found in PTC patients with large nodules or multinodular goiters [10,14]. As a result, several studies have found conflicting results between the prevalence of $BRAF^{V600E}$ mutation in tumor burden and the tumor status or prognosis of patients [4,15,16].

To overcome these limitations, liquid biopsy has demonstrated a potential to provide clinically reliable indications for the diagnosis of PTC, as well as determining its status. Specifically, cell-free DNA (cfDNA) or circulating tumor DNA (ctDNA) has been highlighted as a novel biomarker for the detection of $BRAF^{V600E}$ mutation from thyroid carcinoma. One of the recent studies showed that $BRAF^{V600E}$ mutation status in cfDNA is a good indicator for differentiating patients with thyroid cancer from those with benign tumors [17]. The circulating $BRAF^{V600E}$ mutation status in PTC patients was also found to be associated with tumor aggressiveness, incomplete/indeterminate response rate to treatment, and the existence of lung metastasis [18,19].

Here, using polydopamine-silica (PDA/SiO_2) hybrids as a capture agent for cfDNA, we investigated the diagnostic capability of the $BRAF^{V600E}$ mutation status in cfDNA as a biomarker for PTC. Previously, we developed a novel cfDNA capture system using PDA-SiO_2-coated hydrogel beads, which exhibited high diagnostic capability for colorectal cancer (CRC) and hepatocellular carcinoma (HCC) [20,21]. In this study, we confirmed that our system could improve DNA capture, compared to conventional silica-based capture systems, by combining multiple interactions (PDA-nucleobases+ SiO_2-phosphate backbone) into a single system. The PDA/SiO_2-coated beads were then applied to capture cfDNA from serum samples obtained from 37 patients with PTC. The $BRAF^{V600E}$ mutation was analyzed from captured cfDNA using both conventional and droplet digital polymerase chain reaction (ddPCR). The obtained results were applied for differentiating patients based on the multifocality of tumors since many previous studies have confirmed that high expression of $BRAF^{V600E}$ mutation in cfDNA is strongly correlated with the multifocality [22,23]. The findings presented in this study demonstrate the potential of circulating $BRAF^{V600E}$ mutation as a promising diagnostic biomarker for PTC.

MATERIALS AND METHODS

Experimental details are provided in Supplementary Information.

RESULTS

1. Enhanced DNA Adsorption of PDA/SiO_2 Hybrids

Fig. 1 illustrates the overall process for isolating cfDNA from serum samples obtained from PTC patients, followed by analysis of $BRAF^{V600E}$ mutation status. To synthesize the PDA/SiO_2-coated beads for cfDNA capture, the alginate beads were modified with PDA using EDC/NHS chemistry, followed by SiO_2 coating (See Materials and

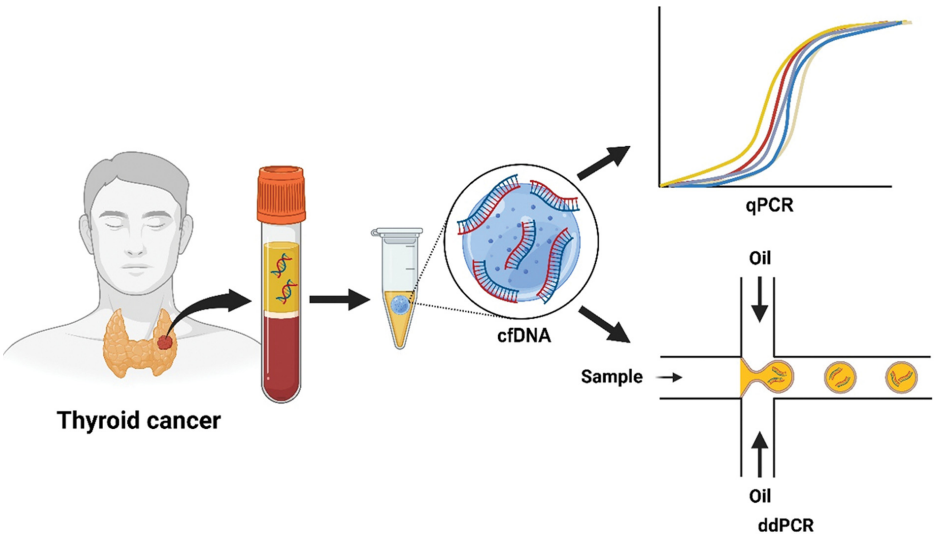

Fig. 1. A schematic diagram illustrating the cfDNA detection using PDA/SiO_2-coated beads from serum samples obtained from PTC patients and the $BRAF^{V600E}$ mutation analysis based on conventional qPCR and ddPCR.

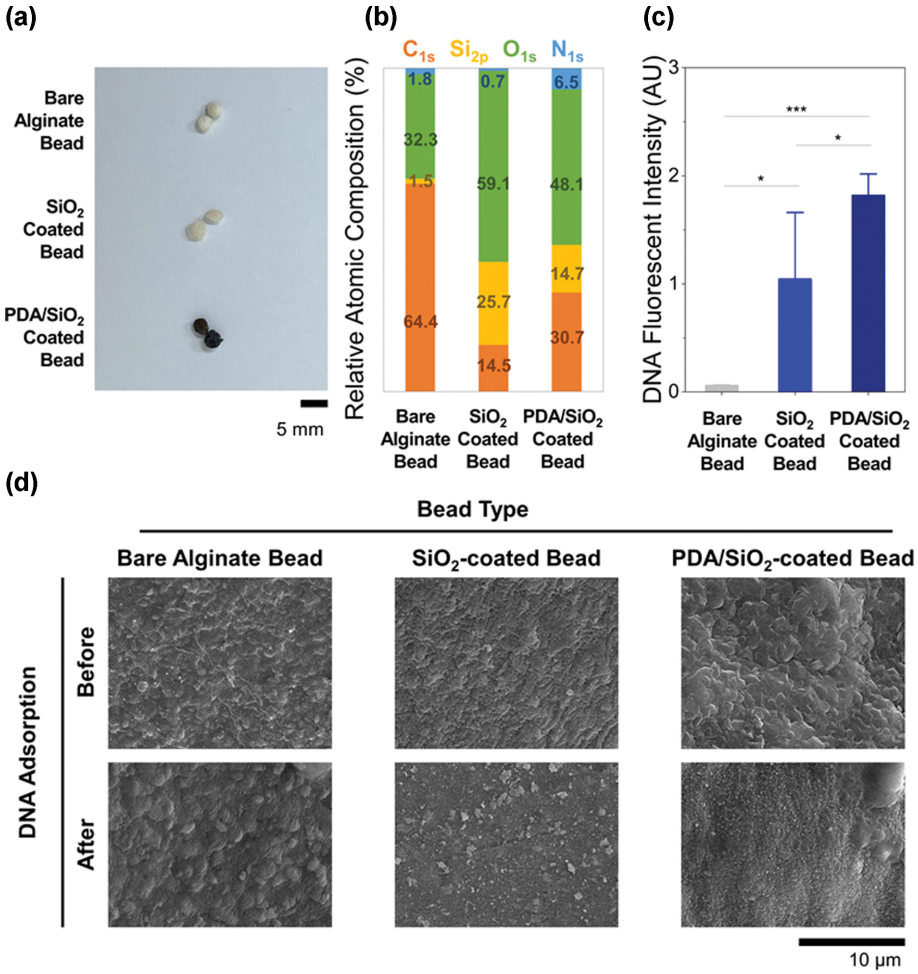

Fig. 2. PDA/SiO_2-coated alginate bead for the enhanced detection of cfDNA: (a) PDA-SiO_2 hybrids were coated sequentially on alginate beads. Note that the images were acquired after the lyophilization. (b) Atomic composition of bare alginate, SiO_2-coated beads, and PDA/SiO_2-coated beads measured using X-ray photoelectron spectroscopy (XPS). (c) The adsorption of DNA on the surface of each bead, measured using fluorescently-labeled DNA. (d) Morphology of the surface of each bead before and after DNA adsorption using scanning electron microscopy (SEM).

Methods for the details). Note that these chemical reactions did not affect the size of the beads. The diameters of the beads coated with SiO_2 and PDA/SiO_2 were 31.1±4.4 mm (p=0.687) and 30.8±2.9 mm (p=0.736), respectively, which showed no significant difference with the diameter of the bare alginate beads (30.3±2.0 mm; Fig. 2(a)). However, significant difference was observed in color between the bare alginate beads and the beads coated with either SiO_2 or PDA/SiO_2. Beads at each step (or type) were further characterized using X-ray photoelectron spectroscopy (XPS) to confirm the surface modification (Fig. 2(b)). The existence of silica on the surface of the alginate bead was evidenced by the significant increase in the ratio of Si_{2p} from SiO_2- or PDA/SiO_2-coated beads, compared to the bare alginate beads. The higher N_{1s} ratio in PDA/SiO_2-coated beads compared to SiO_2-coated beads denotes the presence of PDA.

Prior to clinical application, the cfDNA adsorption of each bead was assessed using the fluorophore-labeled DNA to confirm that PDA/SiO_2 hybrids can capture DNA more efficiently than conventional cfDNA capture systems which use silica alone. After 10 min incubation with fluorescence-labelled DNA, the PDA/SiO_2-coated beads exhibited 1.76-fold (p=0.031) stronger fluorescent signal than SiO_2-coated bead (Fig. 2(c)). This implies that combined interaction between SiO_2-DNA backbone and PDA-nucleobases synergistically increases the adsorption of DNA, which was also demonstrated in our previous studies [20,21]. Note that the fluorescent signal acquired from the bare alginate bead was negligible, indicating that the alginate bead itself does not contribute to cfDNA capture. The surface morphology of beads was analyzed using scanning electron microscopy (SEM), before and after DNA adsorption (Fig. 2(d)). Upon DNA adsorption, nano-sized particles which are presumed to be DNA were observed throughout the surface of PDA/SiO_2-coated beads. The nano-sized particles were also observed from SEM images obtained from SiO_2-coated beads, but the number of these particles was significantly less than that found from PDA/SiO_2-coated beads. In contrast, no remarkable difference was found in the SEM images acquired from the bare alginate beads, before and after DNA adsorption. These findings suggest that our new system improves the capture of cfDNA, which may facilitate the analysis of the $BRAF^{V600E}$ mutation from patients' samples.

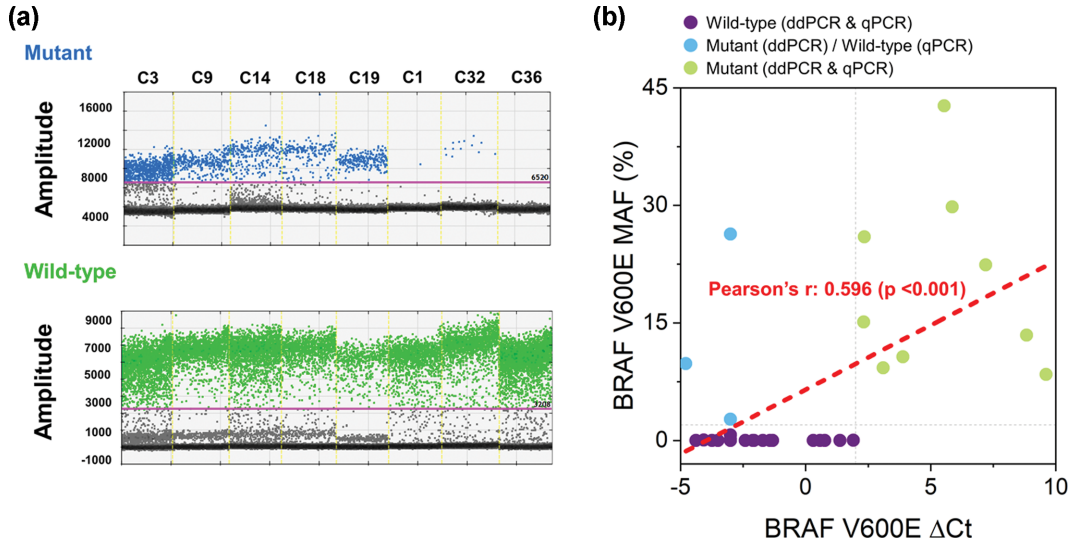

Fig. 3. qPCR and ddPCR assays employed to analyze BRAF^{V600E} mutation from cfDNA isolated from PTC patients. (a) ddPCR for the detection of BRAF^{V600E} mutation. The fluorescence measurement of the mutant probe labeled with 6-fluorescein amidite (FAM) (top) and wild-type probe labeled with hexachlorofluorescein (HEX) (bottom). (b) The correlation between BRAF^{V600E} mutant status measured using qPCR and ddPCR assays.

2. Patient Characteristics

A total of 37 patients with PTC were enrolled in this study. The clinical information of patients enrolled in this study is summarized in Table S1. The majority of patients were women (n=34) and a total of 9 (24.3%), 30 (81.1%), 18 (48.6%), and 16 (43.2%) patients were pathologically confirmed to have multiple tumors, extra-nodal extension, lymphatic invasion (LVI), and lymph node metastasis, respectively. The median tumor size (diameter) of patients was 1.2 cm and ranged from 0.2 to 5.0 cm.

3. Circulating BRAF^{V600E} Mutation Detected Using Conventional qPCR and ddPCR

Both qPCR and ddPCR were utilized to quantify the BRAF^{V600E} mutation status from cfDNA isolated using PDA/SiO_2-coated beads. Briefly, for qPCR the efficiency of peptide nucleic acid (PNA)-mediated PCR clamping was evaluated using threshold cycle (Ct) value, and the difference in Ct value between the sample and control (ΔCt) was utilized for validating the BRAF^{V600E} mutation status. For ddPCR, the percentage of mutant droplets compared to the total (mutant plus wild-type), which is also known as mutation allele frequency (MAF), was calculated to validate the BRAF^{V600E} mutation status (Fig. 3(a)). Note that a commercially available kit (PNA Clamp BRAF^{V600E} mutation detection kit; Panagene, Daejeon, Republick of Korea) was used for the BRAF mutation analysis, which can sensitively detect 0.5% mutation [24].

At the cutoff point of ΔCt≥2, the qPCR assay detected BRAF^{V600E} mutation from a total of nine patients (24.3%) (Table S2). Specifically, an average ΔCt value for patients who had BRAF^{V600E} mutation (ΔCt≥2) was 5.41±2.72, whereas those having lower ΔCt had an average of −2.24±1.73. Meanwhile, the ddPCR assay detected the BRAF^{V600E} mutation from a total of 12 PTC patients (32.4%) at the cutoff point of 2%. At the given cutoff value, patients with BRAF^{V600E} MAF higher and lower than the cutoff exhibited an average MAF of 18.05±11.50% and 0.04±0.14%, respectively. Interestingly, ddPCR assay detected BRAF^{V600E} mutation from all nine patients who were detected to have the mutation by qPCR assay. As a result, the MAF obtained from ddPCR and the ΔCt calculated from qPCR showed a strong correlation, with the Pearson's correlation coefficient of 0.596 ($p<0.001$) (Fig. 3(b)). These findings demonstrate that our cfDNA capture platform can be utilized for both qPCR and ddPCR assays.

4. Clinical Utility of BRAF^{V600E} Mutation Status for the Characterization of PTC

We further analyzed whether the BRAF mutation status validated from cfDNA had an efficient diagnostic capability for differentiating PTC based on its pathological status (Fig. 4(a)). PTC patients with multifocal tumors exhibited significantly higher ΔCt (5.41±1.73) than those having a unifocal tumor (−2.24±2.72; $p<0.001$). The diagnostic accuracy of cfDNA BRAF^{V600E} mutation status to distinguish patients having multifocal PTCs from those having single PTCs was further analyzed. At the given cutoff value (ΔCt≥2), sensitivity, specificity, and accuracy of the BRAF mutation status for differentiating multifocality of PTC were all 100% (Fig. 4(b)). The results obtained from ddPCR also demonstrated a high diagnostic capability for differentiating PTC patients with multifocal tumors from unifocal tumors (19.76±11.49% vs. 1.42±5.24%; $p<0.001$), although the diagnostic performance was not as great as the results obtained from qPCR assay (sensitivity: 100%, specificity: 89.3%, and accuracy: 91.9%). As a result, the receiver operating characteristic (ROC) analysis demonstrated that the BRAF mutation status in cfDNA has a strong correlation with the multifocality of a tumor, with AUC-ROC of 1.000 ($p<0.001$) and 0.946 ($p<0.0001$) for qPCR and ddPCR assays, respectively (Fig. 4(c)). These findings were in good concordance with previous studies that revealed the BRAF mutation is strongly associated with the multifocality of tumors [22,23].

Serum markers that are frequently utilized for determining thyroid functions, such as free thyroxine (Free F4) and thyroid-stimu-

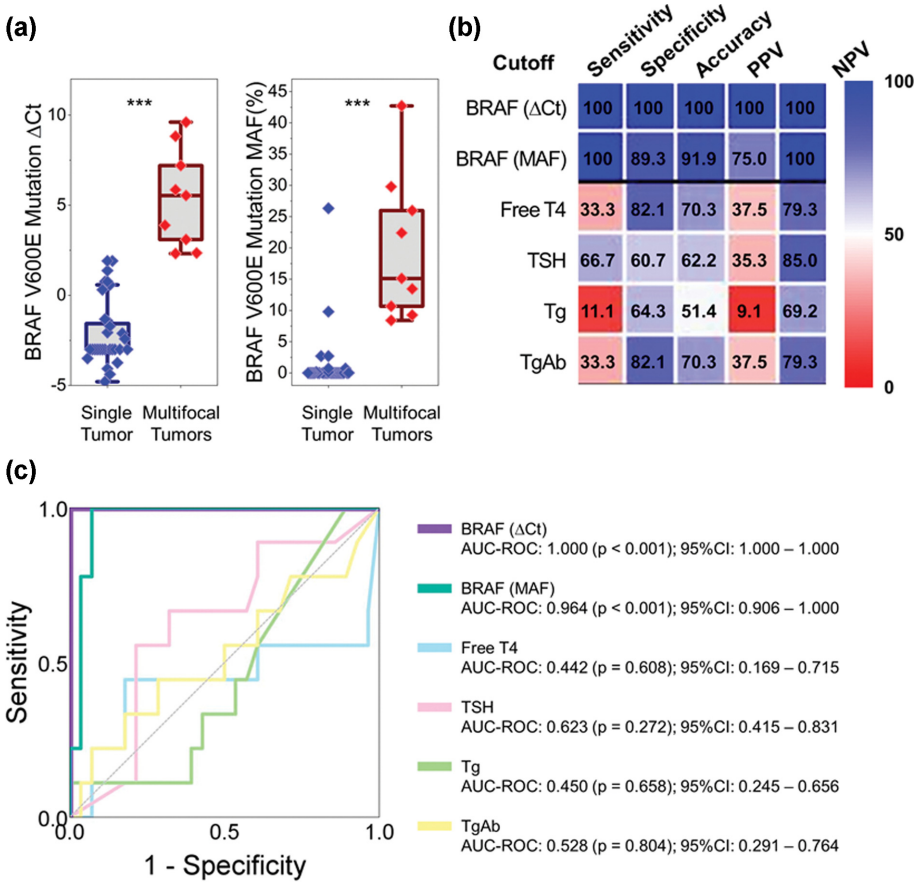

Fig. 4. The correlation between the multifocality of PTC and the BRAF^{V600E} mutation status: (a) The BRAF^{V600E} mutation status depending on the multifocality of PTC; (b) The diagnostic performance of the BRAF^{V600E} mutation status and serum biomarkers for detecting the multifocality of PTC. The cutoff values were 2 for BRAF ΔCt, 2% for BRAF MAF, 1.48 ng/dL for Free T4, 5 U/mL for TSH, 1 IU/mL for Tg, and 4 IU/mL for TgAb; (c) The ROC analysis of the BRAF^{V600E} mutation status and serum biomarkers for detecting the multifocality of PTC.

lating hormone (TSH), as well as those used for characterizing PTCs, such as thyroglobulin (Tg) and antibody against Tg (TgAb), were also quantified from patients' samples. None of these serum proteins effectively diagnosed the multifocality of PTC (statistically insignificant; $p>0.05$). The ROC analysis elicited that these serum biomarkers exhibited AUC-ROC near 0.5 for detecting the multifocality of PTC (Fig. 4(c)).

The BRAF mutation status and serum biomarkers were also employed for detecting extra-nodal extension, LVI, and lymph node metastasis from PTC patients (Table S2). None of these markers exhibited a significant correlation with these pathological features of PTC. However, MAF of BRAF^{V600E} mutation was slightly higher in patients having LVI (2.89±5.93% vs. 9.04±13.51%; $p=0.089$) and nodal metastasis (3.68±7.04% vs. 8.78±13.81%; $p=0.152$). Note that other biomarkers, including ΔCt of BRAF^{V600E} mutation obtained from qPCR, had lower significance than MAF of BRAF^{V600E} mutation for detecting LVI and nodal metastasis.

DISCUSSION

We further processed seven additional samples to check the agreement between BRAF^{V600E} mutation status in the primary tissue and cfDNA. As demonstrated in Table S3, BRAF^{V600E} mutation was not detected in cfDNA from all four patients (including one benign tumor patient) who had BRAF wild-type tumors. Meanwhile, BRAF^{V600E} mutation was detected in two out of three patients in BRAF^{V600E} mutant group. The number of samples used in this study may not be sufficient to conclude that our system provides a good correlation between the BRAF^{V600E} mutation status in tissue and cfDNA. However, we have previously revealed that the gene amplification (HER-2 and AFP) or mutation (KRAS mutation) analyzed in cfDNA shows a strong correlation with that analyzed from the primary tumor [20,21,25].

Tg has been widely utilized to diagnose and characterize PTCs [26,27]. However, Tg had demonstrated poor significance for characterizing and analyzing carcinomas with poor differentiation or de-differentiated tumor [26]. In addition, Tg is not an ideal predictor for estimating the recurrence of a tumor since thyroid tissue remains in the body when lobectomy of isthmusectomy or subtotal lobectomy is performed on thyroid cancer patients. This is one of the reasons why PTC analysis highly relies on imaging or FNA-based biopsy, instead of serum antigen testing.

Specifically, the BRAF mutation has been widely investigated for the analysis of PTCs from biopsy samples obtained from FNAC

(fine needle aspiration cytology). However, as mentioned, BRAF mutation analysis on FNAC samples demonstrated an inaccuracy for the diagnosis of PTC due to the high heterogeneity of tumors [28]. Our study suggests that the BRAF mutation analysis on cfDNA has the potential to overcome these limitations. In particular, our bead-based assay provides sensitive detection of cfDNA from human serum samples, which can facilitate the BRAF mutation analysis in cfDNA. This was evidenced by our previous studies, as PDA/SiO_2-coated beads not only adsorbed cfDNA more effectively from human samples but also detected cancer-associated genes more accurately than commercially available DNA analysis kits [21,25]. This study also supports that our system can be applied for the detection of BRAF mutation from PTC patients, which has the potential to accurately predict the characteristics of PTC. Moreover, our system can be further applied for detecting other types of genetic alterations. Based on these analyses, we can collect a set of genes that are strongly associated with high-risk pathological features of PTC and develop a cfDNA gene panel for the accurate diagnosis of the tumor.

CONCLUSION

FNA-based tissue analysis or the detection of thyroid-associated serum antigens has demonstrated a low sensitivity for identifying PTC. Thus, there is an urgent need to establish a clinically reliable biomarker for the analysis of PTC. In this study, we utilized PDA/SiO_2-coated beads for the capture of cfDNA from human blood and analyzed the BRAF mutation status to differentiate PTC patients based on the pathological features of the tumor. Specifically, we demonstrated that our system adsorbs cfDNA more efficiently than the conventional silica-based cfDNA detection systems (1.76-fold increased DNA detection; p=0.031). Using the DNA collected from the beads, we analyzed the BRAF mutation status from 37 PTC patients based on both qPCR and ddPCR. The results acquired from both assays revealed that the BRAF mutation status is strongly associated with the multifocality of tumors. Meanwhile, none of the serum biomarkers have demonstrated clinical significance for detecting multifocality or other malignancies in PTC. These findings imply that our cfDNA capture system can be applied for the analysis of various mutations in PTC, which can be employed as a reliable diagnostic biomarker for PTC.

ACKNOWLEDGEMENT

This work was supported by Basic Science Research Program Funded by Ministry of Science and Technology (Republic of Korea) under grant # NRF-2022R1F1A1075414. It has been also partially supported by NRF under grant # NRF-2020R1A2C4001856/#NRF-2019M3E5D1A02068557, KHIDI under grant #HR20C0025040021, Chungnam National University Hospital Research Fund 2019, the Leaders in Industry-university Cooperation 3.0 Project, and the National Research Foundation of Korea Grant funded by the Korean Government(MOE).

CONFLICT OF INTEREST

The authors declare no conflict of interest.

SUPPORTING INFORMATION

Additional information as noted in the text. This information is available via the Internet at http://www.springer.com/chemistry/journal/11814.

REFERENCES

1. A. Miranda-Filho, J. Lortet-Tieulent, F. Bray, B. Cao, S. Franceschi, S. Vaccarella and L. Dal Maso, *Lancet Diabetes Endocrinol.*, **9**(4), 225 (2021)
2. J. Ferlay, M. Colombet, I. Soerjomataram, D. M. Parkin, M. Piñeros, A. Znaor and F. Bray, *Int. J. Cancer*, Online ahead of print (2021).
3. B. R. Haugen, E. K. Alexander, K. C. Bible, G. M. Doherty, S. J. Mandel, Y. E. Nikiforov, F. Pacini, G. W. Randolph, A. M. Sawka, M. Schlumberger, K. G. Schuff, S. I. Sherman, J. A. Sosa, D. L. Steward, R. M. Tuttle and L. Wartofsky, *Thyroid*, **26**(1), 1 (2016)
4. A. Prete, P. Borges de Souza, S. Censi, M. Muzza, N. Nucci and M. Sponziello, *Front. Endocrinol.*, **11**, 102 (2020).
5. M. Xing, W. H. Westra, R. P. Tufano, Y. Cohen, E. Rosenbaum, K. J. Rhoden, K. A. Carson, V. Vasko, A. Larin, G. Tallini, S. Tolaney, E. H. Holt, P. Hui, C. B. Umbricht, S. Basaria, M. Ewertz, A. P. Tufaro, J. A. Califano, M. D. Ringel, M. A. Zeiger, D. Sidransky and P. W. Ladenson, *J. Clin. Endocrinol. Metab.*, **90**(12), 6373 (2005).
6. M. Xing, A. S. Alzahrani, K. A. Carson, Y. K. Shong, T. Y. Kim, D. Viola, R. Elisei, B. Bendlová, L. Yip, C. Mian, F. Vianello, R. M. Tuttle, E. Robenshtok, J. A. Fagin, E. Puxeddu, L. Fugazzola, A. Czarniecka, B. Jarzab, C. J. O'Neill, M. S. Sywak, A. K. Lam, G. Riesco-Eizaguirre, P. Santisteban, H. Nakayama, R. Clifton-Bligh, G. Tallini, E. H. Holt and V. Sýkorová, *J. Clin. Oncol.*, **33**(1), 42 (2015).
7. M. Xing, A. S. Alzahrani, K. A. Carson, D. Viola, R. Elisei, B. Bendlova, L. Yip, C. Mian, F. Vianello, R. M. Tuttle, E. Robenshtok, J. A. Fagin, E. Puxeddu, L. Fugazzola, A. Czarniecka, B. Jarzab, C. J. O'Neill, M. S. Sywak, A. K. Lam, G. Riesco-Eizaguirre, P. Santisteban, H. Nakayama, R. P. Tufano, S. I. Pai, M. A. Zeiger, W. H. Westra, D. P. Clark, R. Clifton-Bligh, D. Sidransky, P. W. Ladenson and V. Sykorova, *Jama*, **309**(14), 1493 (2013).
8. J. Ge, J. Wang, H. Wang, X. Jiang, Q. Liao, Q. Gong, Y. Mo, X. Li, G. Li, W. Xiong, J. Zhao, Z. Zeng and J. Ge, *J. Cancer*, **11**(4), 932 (2020).
9. R. Elisei, D. Viola, L. Torregrossa, R. Giannini, C. Romei, C. Ugolini, E. Molinaro, L. Agate, A. Biagini, C. Lupi, L. Valerio, G. Materazzi, P. Miccoli, P. Piaggi, A. Pinchera, P. Vitti and F. Basolo, *J. Clin. Endocrinol. Metab.*, **97**(12), 4390 (2012).
10. M. Mekel, H. Gilshtein, A. Al-Kurd, B. Bishara, M. M. Krausz, H. R. Freund, Y. Kluger, A. Eid and H. Mazeh, *World J. Surg.*, **40**(1), 124 (2016).
11. S. R. Orell, *Cytopathology*, **14**(4), 173 (2003).
12. R. Abi-Raad, M. Prasad, R. Baldassari, K. Schofield, G. G. Callender, D. Chhieng and A. J. Adeniran, *Endocr. Pathol.*, **29**(3), 269 (2018).
13. X. M. Yu, P. N. Patel, H. Chen and R. S. Sippel, *Am. J. Surg.*, **203**(3), 331 (2012).
14. M. J. Campbell, C. D. Seib, L. Candell, J. E. Gosnell, Q. Y. Duh, O. H. Clark and W. T. Shen, *World J. Surg.*, **39**(3), 695 (2015).
15. A. Finkel, L. Liba L, E. Simon, T. Bick, E. Prinz, E. Sabo, O. Ben-

Izhak and D. Hershkovitz, *J. Clin. Endocrinol. Metab.*, **101**(4), 1407 (2016).
16. A. Guerra, M. R. Sapio, V. Marotta, E. Campanile, S. Rossi, I. Forno, L. Fugazzola, A. Budillon, T. Moccia, G. Fenzi and M. Vitale, *J. Clin. Endocrinol. Metab.*, **97**(2), 517 (2012).
17. C. Pupilli, P. Pinzani, F. Salvianti, B. Fibbi, M. Rossi, L. Petrone, G. Perigli, M. L. De Feo, V. Vezzosi, M. Pazzagli, C. Orlando and G. Forti, *J. Clin. Endocrinol. Metab.*, **98**(8), 3359 (2013).
18. K. Jensen, S. Thakur, A. Patel, M. C. Mendonca-Torres, J. Costello, C. J. Gomes-Lima, M. Walter, L. Wartofsky, K. D. Burman, A. Bikas, D. Ylli, V. V. Vasko and J. Klubo-Gwiezdzinska, *J. Clin. Med.*, **9**(8), 2481 (2020).
19. B. H. Kim, I. J. Kim, B. J. Lee, J. C. Lee, I. S. Kim, S. J. Kim, W. J. Kim, Y. K. Jeon, S. S. Kim and Y. K. Kim, *Yonsei Med. J.*, **56**(3), 634 (2015).
20. T. Lee, P. A. Rawding, J. Bu, S. Hyun, W. Rou, H. Jeon, S. Kim, B. Lee, L. J. Kubiatowicz, D. Kim, S. Hong and H. Eun, *Cancers*, **14**(9), 2061 (2022).
21. J. Bu, T. H. Lee, W. J. Jeong, M. J. Poellmann, K. Mudd, H. S. Eun, E. W. Liu, S. Hong and S. H. Hyun, *PloS One*, **15**(12), e0242145 (2020).
22. H. Z. Kimbrell, A. B. Sholl, S. Ratnayaka, S. Japa, M. Lacey, G. Carpio, P. Bhatia and E. Kandil, *BioMed. Res. Int.*, **2015**, 486391 (2015).
23. C. Li, K. C. Lee, E. B. Schneider and M. A. Zeiger, *J. Clin. Endocrinol. Metab.*, **97**(12), 4559 (2012).
24. D. Jeong, Y. Jeong, J. H. Park, S. W. Han, S. Y. Kim, Y. J. Kim, S. J. Kim, Y. Hwangbo, S. Park, H. D. Cho, M. H. Oh, S. H. Yang and C. J. Kim, *Ann. Surg. Oncol.*, **20**(3), 759 (2013).
25. J. Bu, T. H. Lee, M. J. Poellmann, P. A. Rawding, W. J. Jeong, R. S. Hong, S. H. Hyun, H. S. Eun and S. Hong, *Clin. Transl. Med.*, **11**(8), e499 (2021).
26. M. Prpić, M. Franceschi, M. Romić, T. Jukić and Z. Kusić, *Acta Clinica Croat.*, **57**(3), 518 (2018).
27. B. S. H. Indrasena, *World J. Biol. Chem.*, **8**(1), 81 (2017).
28. C. K. Zhao, J. Y. Zheng, L. P. Sun, R. Y. Xu, Q. Wei and H. X. Xu, *Cancer Med.*, **8**(12), 5577 (2019).

Supporting Information

A high-sensitivity cfDNA capture enables to detect the BRAF V600E mutation in papillary thyroid carcinoma

Tae Hee Lee*,,‡, Hong Jae Jeon***,‡, Jung Hyun Choi****,‡, Young Jun Kim*****, Pil-Neo Hwangbo**, Hyun Sung Park****, Chae Yeon Son****, Hei-Gwon Choi******,*******, Ha Neul Kim******,*******, Jae Won Chang********, Jiyoon Bu****,*********,†, and Hyuk Soo Eun*********,**********,†**

*Department of Biomedical Laboratory Science, Daegu Health College, Chang-ui Building, 15 Yeongsong-ro, Buk-gu, Daegu 41453, Korea
**Industry Academic Cooperation Foundation, Daegu Health College, 15 Yeongsong-ro, Buk-gu, Daegu 41453, Korea
***Department of Internal Medicine, Chungnam National University Sejong Hospital (CNUSH), 20, Bodeum 7-ro, Sejong 30099, Korea
****Department of Biological Sciences and Bioengineering, Inha University, 100 Inha-ro, Michuhol-gu, Incheon 22212, Korea
*****School of Integrative Engineering, Chung-Ang University, Heukseok-dong, Dongjak-gu, Seoul 06974, Korea
******Brain Korea 21 FOUR Project for Medical Science, Chungnam National University, 266, Munwha-ro, jung-gu, Daejeon 35015, Korea
*******Department of Medical Science, Chungnam National University, 266, Munwha-ro, jung-gu, Daejeon 35015, Korea
********Department of Otolaryngology-Head and Neck Surgery, Research Institute for Medical Science, Chungnam National University, 266, School of Medicine, Daejeon 35015, Korea
*********Industry-Academia Interactive R&E Center for Bioprocess Innovation, Inha University, Incheon 22212, Korea
**********Department of Internal Medicine, Chungnam National University Hospital, 282, Daejeon 35015, Korea
**********Department of Internal Medicine, College of Medicine, Chungnam National University, 266, Munwha-ro, jung-gu, Daejeon 35015, Korea
(*Received 1 August 2022 • Revised 12 November 2022 • Accepted 16 November 2022*)

MATERIALS AND METHODS

1. Surface Engineering of Alginate Beads with PDA-SiO_2-Functionalized Beads

Sodium alginate (5% w/v) was dissolved in distilled water (DW) and then dropped into 100 mM calcium chloride aqueous solution (1 h, room temperature (RT)). The alginate beads were carefully washed three times by DW. The carboxylic groups on the alginate beads were activated using EDC/NHS chemistry. The beads were treated with 200 mM EDC and 200 mM NHS in ddH_2O at room temperature for 1 h. For the PDA-SiO_2-immobilized beads, alginate beads were substantially reacted with dopamine hydrochloride and silica. In brief, dopamine hydrochloride (5 mM) was added into the bead-containing solution dropwise and stirred at room temperature for 12 h. The acidity of the dopamine hydrochloride solution was maintained at a pH of ~7.0 using Tris-HCl buffer. The dopamine-functionalized beads were then washed with DW three times (1 min for each) and mixed with 1 mL silica solution for 1 h in RT.

2. Surface Characterization Using XPS

The chemical composition of the beads was identified by the Themo Scientific K-Alpha XPS system. Survey spectra were collected over a range of 0-1,200 eV with a pass energy of 100.0 eV and a step of 1.0 eV. High-resolution spectra of C_{1s}, O_{1s}, N_{1s}, and Si_{2p} were also collected under adjusted conditions. Each measurement was repeated five times.

3. The extraction of Circulating Tumor DNA (ctDNA) Using PDA-SiO_2-functionalized Beads

The patient samples were provided by the National University Hospital biobank of Chungbuk, a member of the Korea Biobank Network. This study was proved by the Institutional Review Board of Chungnam National University Sejong Hospital (CNUSH-20-11-012) and Chungnam National University Hospital (CNUH-2019-07-041-013). The pre-treatment process for ctDNA extraction of the sample is as follows: 200 μL buffy coat was obtained from 3 ml whole blood after the lysis of erythrocyte using erythrocyte lysis (EL) buffer (Qiagen, Inc., Hilden, Germany). 1,500 μL of EL buffer was added into 300 μL of buffy coat and then incubated for 15 min at 4 °C. After incubation, the sample was centrifuged at 400 g for 10 min at 4 °C, which was repeated twice each after the discard of supernatants. The cell pellet was treated with 20 μL of proteinase K and 200 μL AL buffer (Qiagen, Inc., Hilden, Germany) and incubated at 37 °C for 10 min, followed by the reaction with 200 μL of 95% ethanol (Samchun, Seoul, Korea). A PDA-SiO_2-functionalized bead was then added to the sample with 5 μL calcium chloride solution, followed by the incubation under gentle agitation (10 min). The beads were washed with an AW1 buffer (Qiagen, Inc., Hilden, Germany) and stored in RNase/DNase free water at −80 °C.

4. DNA Capture Capability Analysis Using Fluorophore-labeled DNA

The beads were incubated with fluorophore-labeled DNA (50 ng/μL; 200 μL) which consists of a mixture of RPP30 forward primer

(5′FAM-GATTTGGAC CTGCGAGCG-3′) 5-FAM-GATTTGGAC CTGCGAGCCG-3) and RPP30 reverse primer (5′FAM-GCG-GCTGTCTCCACAAGT-3′) for 30 min, followed by washing the beads with AW1 buffer. Beads were then kept in 200 μL elution buffer. Fluorescent intensity of the captured DNA was then analyzed using a plate reader (Varioskan LUX Plate Reader; Thermo Fisher Scientific) at the excitation of 500 nm.

5. Quantitative Polymerase Chain Reaction (qPCR) and Droplet Digital PCR (ddPCR) Workflow

PNA Clamp BRAF^{V600E} mutation detection kit (Panagene, Daejeon, Republic of Korea) was used, according to the manufacturer's instructions. Briefly, all reactions were performed in a final volume of 20 μL that contains 1 μL DNA, 6 μL DW, 3 μL BRAF mix, 10 μL 2X premix, primers, and PNA probes for codon 600. The PNA-clamping PCR was performed using a CFX96 real-time PCR system (BioRad, Pleasanton, CA). The PCR cycling conditions were at 94 °C for 5 minutes, followed by 40 cycles of amplification at 94 °C for 30 seconds, 70 °C for 20 seconds, 63 °C for 30 seconds, and a final extension at 72 °C for 5 minutes. The threshold cycle (Ct) was automatically calculated by observing the SYBR Green amplification plots. The delta-Ct (ΔCt) values were calculated as ([Control Ct]−[Sample Ct]=ΔCt). A cut-off value of 2.0 was used for determining the presence of BRAF mutant DNA. The ddPCR (QX200, Bio-Rad, Hercules, CA, USA) was used in this study. We prepared 20 μL aliquots of ddPCR reaction mixture consisting of DNA (2 μL), 2x ddPCR supermix for probes (10 μL), 20× BRAF^{V600} screening assay (1 μL), and DW (7 μL). The mixture was loaded to a disposable droplet generator cartridge. After droplet generation was completed, the droplets were transferred to the thermal cycler (Bio-Rad, T100) under the following conditions: 95 °C for 10 min (1 cycle); 94 °C for 30 s and 55 °C for 1 min (40 cycles); 55 °C for 1 min, 98 °C for 10 min (1 cycle), 4 °C hold. Cycled droplets were read individually with the QX200 droplet-reader. The QuantaSoft™ software was analyzed to determine the amount of the target DNA in copies/μL. The mutant allele fraction (MAF) was calculated by dividing the number of droplets containing mutants by the total number of droplets.

6. Statistics

The expression levels of serum biomarkers (i.e., free T4, Thyroid stimulating hormone (TSH), Thyroglobulin (Tg), and Thyroglobulin antibody (TgAb), as well as the BRAF mutation status was compared depending on the tumor multifocality based on Student's *t* test. The correlations between ddPCR and qPCR were analyzed using Pearson correlation and linear regression models. Clinical capabilities were further assessed by the receiver operating characteristic (ROC) analysis. All statistical analyses were made through SPSS Statistics 26 (SPSS, IL).

Table S1. Clinical information of PTC patients involved in this study

	Median	Range
Height (cm)	157	131.6-170
Weight (kg)	64.2	36.9-87
	Male	Female
Gender	3 (8.1%)	34 (91.9%)
	Y	N
Multifocality	9 (24.3%)	28 (75.7%)
Lymph node metastasis	16 (43.2%)	21 (56.8%)
Lymphatic invasion	18 (48.6%)	19 (51.4%)
Extranodal extension	30 (81.1%)	7 (18.9%)

Table S2. The BRAF mutation status and serum antigens for differentiating pathological features of PTC

	BRAF ΔCt (AU)	BRAF MAF (%)	Free T4 (ng/dL)	TSH (U/mL)	Tg (IU/mL)	TgAb (IU/mL)
Multifocality (N vs. Y)	−2.24±1.73 vs 5.41±2.72 (p<0.001)	1.42±5.24 vs 19.76±11.49 (p<0.001)	1.15±0.49 vs 0.85±0.81 (p=0.306)	28.29±41.04 vs 48.27±41.97 (p=0.215)	0.90±1.19 vs 1.10±2.61 (p=0.752)	5.80±16.32 vs 10.18±22.00 (p=0.524)
Extra nodal exten. (N vs. Y)	−1.31±2.56 vs −0.16±4.12 (p=0.484)	3.56±6.27 vs 6.42±11.45 (p=0.530)	1.14±0.39 vs 1.07±0.63 (p=0.767)	35.96±47.51 vs 32.50±40.97 (p=0.846)	0.66±1.01 vs 1.02±1.72 (p=0.595)	10.56±25.27 vs 6.00±15.81 (p=0.546)
LVI (N vs. Y)	−0.77±3.92 vs 0.04±3.88 (p=0.529)	2.89±5.93 vs 9.04±13.51 (p=0.089)	1.06±0.54 vs 1.10±0.65 (p=0.836)	27.92±38.58 vs 38.67±45.00 (p=0.440)	0.79±1.28 vs 1.12±1.91 (p=0.543)	2.36±2.53 vs 11.62±24.60 (p=0.130)
Lymph node meta. (N vs. Y)	−1.13±3.31 vs 0.61±4.41 (p=0.180)	3.68±7.04 vs 8.78±13.81 (p=0.152)	1.14±0.57 vs 1.00±0.62 (p=0.503)	30.89±42.51 vs 36.13±41.54 (p=0.710)	0.92±1.81 vs 1.00±1.35 (p=0.878)	5.88±14.60 vs 8.16±21.43 (p=0.702)

* For Free T4, the patients exhibiting serum Free T4 level lower than the detection limit (0.4) were considered to have 0 ng/dL Free T4

** For TSH, the patients exhibiting serum TSH level higher than the detection limit (100.00) were assigned to have 100 U/mL TSH

Table S3. The BRAF mutation status in cfDNA and the primary tissue. Note that the BRAF mutation in the primary tissue was determined by pathological analysis reported by Chungnam National University Hospital. Note that the results obtained from cfDNA and tissue samples matched for six out of seven patients (bold)

Sample ID	Tumor status	cfDNA		Tissue
		ΔCt	Mutant/Wild	Mutant/Wild
P00S1	**PTC**	**6.56**	**Mutant**	**Mutant**
P00S2	PTC	−1.52	Wild	Mutant
P00S3	**PTC**	**3.87**	**Mutant**	**Mutant**
P00S4	**PTC**	**0.45**	**Wild**	**Wild**
P00S5	**PTC**	**−5.00**	**Wild**	**Wild**
P00S6	**PTC**	**−5.00**	**Wild**	**Wild**
P00S7	**Benign**	**−3.04**	**Wild**	**Wild**